In situ U–Pb zircon micro-geochronology of MCT zone rocks in the Lesser Himalaya using LA–MC–ICPMS technique

P. K. Mukherjee*, Saurabh Singhal, Vikas Adlakha, S. K. Rai, Som Dutt, Aditya Kharya and A. K. Gupta

Wadia Institute of Himalayan Geology, 33, General Mahadeo Singh Road, Dehradun 248 001, India

A multi-collector (MC) inductively coupled plasma mass spectrometer (ICPMS) was used in combination with an Excimer (193 nm) laser to carry out *in situ* U–Pb dating of zircons. High performance two-volume sample cell provided unmatched laser ablated aerosol transportation efficiency resulting in reducing laser-related down-hole fractionation. Three well-characterized natural zircon reference standards (Harvard zircon 91500, GJ-1 zircon, Plešovice) were repeatedly measured in different sessions to evaluate the analytical figures of merits. Precision of <1% was achieved for spot sizes 20 μm with accuracies well within 2% of the reference values for these standards. Zircons from MCT Zone in the inner Lesser Himalaya reveal a highly discordant Palaeo-proterozoic (1901 ± 11 Ma) magmatic crystallization age inferred from the upper intercept in the concordia plot. The $^{207}Pb/^{206}Pb$ ages are also internally consistent with the disconcordia age with a weighted mean of 1900 ± 10 Ma and in turn suggest a major phase of Palaeo-proterozoic magmatic activity along the northern margin of Indian craton, while Early Miocene (~25 Ma) Pb loss in zircon inferred from lower intercept in disordria may be related to tectono-thermal activity along MCT.

Keywords: LA–MC–ICPMS, Lesser Himalaya, MCT zone, U–Pb geochronology, zircon.

Since the introduction of commercially available inductively coupled (argon) plasma (ICP) in the early 1970s as one of the most efficient sources of ionization, applications of mass spectrometry (MS) in earth science have grown exponentially. Further, ICPMS coupled with laser ablation (LA) as micro-sampling device, facilitates *in situ* isotopic analysis at high spatial resolution keeping the textural relationship of the sample intact, allowing better control on data interpretation. The technique provides an up-to-date advancement in wide-ranging geological applications that require trace elemental analysis, isotopic composition and radiometric dating at microscopic scale[1–5] to decipher the earth's evolution and dynamics. High throughput, cost-effectiveness and high accuracy and precision are major advantages of LA–multi-collector (MC)-ICPMS technique.

The major drawbacks of ICP as ion source are: (i) polyatomic interferences and (ii) plasma-related flickers that seriously affect the accuracy and precision of measurements[6] in comparison to thermal ionization mass spectrometers (TIMS). However, flicker in plasma has been circumvented through simultaneous measurement by introducing MC configuration. Thus, MC-ICPMS has the dual advantages of high resolution similar to TIMS and high ionization efficiency of ICP source[7], which makes it the best suited and cost-effective technique for micro-geochronology[5].

Zircon ($ZrSiO_4$) is a chemically inert and refractory accessory mineral which can survive both weathering and transport processes as well as high temperature metamorphism and anatexis. It survives not only under extreme conditions, but grows during these natural thermal events and thus, each individual crystal, or parts of that crystal, may therefore have a different origin[8,9]. Therefore, the mineral records the processes of multiphase tectono-metamorphic events witnessed since origin[10]. Zircon is omnipresent in silicate rocks and invariably contains variable amount of U ranging from tens to thousands of μg/g, which makes these tiny grains suitable for the U–Pb dating[7–12].

In this study, analytical merits of U–Pb micro-dating of zircon are evaluated using a 193 nm Ar–F Excimer laser source for *in situ* micro-sampling coupled to a MC double-focusing ICPMS for precise measurements of isotope ratios at the newly installed state-of-the-art LA–MC-ICPMS at the Wadia Institute of Himalayan Geology (WIHG), Dehra Dun. Accuracy and precision of the technique were validated by measuring well-characterized natural zircon standards, viz. Harvard 91500 (ref. 13), GJ-1 (ref. 11) and Plešovice[14] and comparing them with reference values. Optimization of instrumental parameters has also been addressed for enhanced sensitivity, ablation-related elemental fractionation and signal response. The analytical protocol was further verified through measurement of natural zircons from a mylonitic gneissic sample in the proximity of Main Central Thrust (MCT)

*For correspondence. (e-mail: mukherjeepkddn@gmail.com)

Table 1. Optimized instrumental parameters for multi-collector (MC) inductively coupled plasma mass spectrometer (ICPMS) and laser ablation (LA) system in this study

LA system (analyte G2; Photon Machines)		MC-ICPMS (Neptune Plus, Thermo Fisher Scientific)	
Type		Cool gas	16 l/min
Laser	Excimer 193 nm	Auxiliary gas	0.7 l/min
Repetition rate	5 Hz	Sample gas	0.931 l/min
Energy density	4 Jcm^{-2}	RF power	1350 W
Spot size (μm)	35, 20, 15 and 8	Detector mode	Mixed Faraday + ICs
Helium carrier gas	0.9 l/min	Integration Time	0.5 sec/cycle
Shot count	150	Scan mode	Static
Masses measured	Detector: IC5, IC4, IC2, IC1B, IC6, H3, H4		
	Mass: ^{202}Pb, ^{204}Hg, ^{206}Pb, ^{207}Pb, ^{208}Pb, ^{232}Th, ^{238}U		

within the intensely deformed shear zone on footwall side in the inner Lesser Himalaya, known as MCT zone (MCTZ) or Munsiari Formation, for which enough published data are available for comparison.

Experimental

The Harvard 91500 is a gem-quality large zircon crystal and a fragment of this crystal is used as primary standard. The ID-TIMS date of this zircon is 1062.32 ± 2.2 Ma (ref. 13). The GJ-1 is also a fragment from a gem-quality larger zircon, provided by the Australian Research Council Centre, Macquarie University, Sydney, and is well-established for a precise TIMS U–Pb age of 601 ± 4 Ma using ID-TIMS technique[11]. The Plešovice zircons are moderate-sized metamorphic crystals, extracted from potassic granulite, having ID-TIMS concordant age of 337.13 ± 0.37 Ma (ref. 14). All three zircon grains were mounted on epoxy resin in either 2.5 cm circular block or on glass slides and finely polished down to 0.5 μm using diamond suspension. A gneissic mylonite sample belonging to Munsiari Formation of the Lesser Himalaya (collected near Joshimath) were processed for extraction using standard crushing, grinding, and gravity and magnetic separation protocol. Zircon grains were picked under microscope and mounted on epoxy resin mounts and polished. Cathodoluminescence (CL) images were obtained to mark the core and rim zones for each of the samples that helps in selecting the spot for U–Pb measurements.

The LA–MC-ICPMS instrumental set-up consists of the MC-ICPMS (Neptune-plus) and an Ar–F Excimer LA system (193 nm UV laser, Cetec-Photon Machine Inc), equipped with high performance HelEx-II active two-volume sample chamber. High-purity helium was used as carrier gas (0.9 l/min) to extract ablated aerosol and introduced into the plasma interface. Four laser spot sizes of 35, 20, 15 and 8 μm were chosen in the present experiment; however, for MCTZ zircon, only 20 μm spot size was used. A burst count of 150 gives about 30 sec of ablation that makes a crater depth of about 12–15 μm ensuring at least 20–25 sec of useful stable signal consisting of more than 40 cycles of integration per measurement. Table 1 provides details of instrumental parameters and detector cup-configuration.

U–Pb systematics and zircon geochronology

Multi-collector detection of U, Th and Pb isotopes allows three geochronometer decay schemes ($^{238}U \rightarrow {}^{206}Pb$, $^{235}U \rightarrow {}^{207}Pb$ and $^{232}Th \rightarrow {}^{208}Pb$) that can be simultaneously used for dating the U–Th-rich accessory minerals such as zircon, monazite, apatite, etc. The validity of measurement is confirmed through the convergence of all these three dates. However, in $^{232}Th \rightarrow {}^{208}Pb$ decay scheme, ^{230}Th is an intermediate daughter product that often disturbs the secular equilibrium leading to erroneous results and is rarely used in zircon geochronology[15]. There is yet another geochronometer that is derived from the first two schemes, i.e. $^{207}Pb/^{206}Pb$. Since common lead contribution in zircon is considered to be negligible, simplified classical U–Pb age equations are as follows

$$\left(\frac{^{206}Pb*}{^{238}U}\right) = (e^{\lambda_{238}t} - 1), \tag{1}$$

$$\left(\frac{^{207}Pb*}{^{235}U}\right) = (e^{\lambda_{235}t} - 1), \tag{2}$$

$$\left(\frac{^{207}Pb*}{^{206}U}\right) = \frac{1}{137.88}\frac{(e^{\lambda_{235}t} - 1)}{(e^{\lambda_{238}t} - 1)}, \tag{3}$$

where Pb* is radiogenic Pb and λ_{238} and λ_{235} the decay constants of ^{238}U and ^{235}U respectively. In case of zircons with low U content or those that are younger than 1.2 Ga, radiogenic Pb is very low and consequently error of estimation is likely to be large resulting in erroneous $^{207}Pb/^{206}Pb$ age[15,16]. However, for older zircons, the $^{207}Pb/^{206}Pb$ age (eq. 3) is more preferred as it is insensitive to recent Pb loss. The decay constant for ^{238}U is after Jaffey *et al.*[17], while that of ^{235}U is derived from λ_{238}, assuming constant abundance of $^{238}U/^{235}U$ ratio (137.818 ± 0.045)[18,19].

Measurement strategies: standard bracketing

The instrumental conditions were tuned under solution mode first for optimum sensitivity for ^{238}U to about 65 volts per μg/g (ppm). This was followed by LA-related optimization, i.e. He gas flow, repetition rates and fluence of the laser energy using NIST 610 and NIST 612 glass standards at various spot sizes to maximize the sensitivity and minimize elemental fractionation at laser excavation site. Ionization efficiency is affected if the oxide formation and presence of doubly charged ions are high. Plasma condition optimization included minimization of ThO/Th and Ba^{++}/Ba to <1% of net Th and Ba signal respectively. Since abundances of radiogenic Pb isotopes and ^{235}U are in the order of magnitude lower than the ^{238}U and ^{232}Th, the former isotopes were measured by more sensitive ion counters (ICs).

In all sessions of measurements, Harvard zircon 91500 was used as primary standard for normalization; the other two zircon standards (GJ-1 and Plešovice) and MCTZ zircons were measured by bracketing with intermittent measurements of standard zircon 91500 to account for instrumental drift, isotopic fractionation and mass bias.

Off-line data reduction

The data file from the mass spectrometer was retrieved into 'IOLITE' (version 2.5)[20] for off-line processing. Gas blank signal between two analyses (excluding washout time) was used as baseline as a series of analyses progress in a session. The net signal time slice was selected through visualization of the peak intensities that are free from any memory effect and initial spiked signal. Once the baseline and sample signal slices were chosen for different samples, U–Pb data reduction scheme (DRS) was invoked by choosing appropriate parameters such as reference standard normalization, down-hole fractionation correction, common lead correction and threshold significant signal. Various plots and statistics of the processed data were done using VisualAge[21] (integrated with IOLITE) and ISOPLOT (ref. 22).

Results and discussion

Multiple measurements on standard zircon samples were made at four different spot sizes (35, 20, 15 and 8 μm) over four different sessions under optimized conditions and instrumental set-up (Table 1). All the three reference zircons are well characterized and have wide range of U concentration (70 to >1000 ppm) and age (337–1065 Ma). This is appropriate to validate the technique that can be implemented in routine measurement of a wide variety of natural zircons such as MCTZ zircons. Analytical figures of merit of the experiment are discussed in terms of accuracy and precision. U–Pb dating by LA–MC-ICPMS of zircons is generally carried out at spot size of about 25 μm. However, it is often desired to carry out the analysis at higher spatial resolution to clearly resolve the thin growth zones in zircon. Keeping this in mind, smaller spot sizes (20, 15 and 8 μm) were also studied to optimize the minimum spot size that can be employed with reasonable precision. However, the results of 8 μm are not up to the mark as the down-hole fractionation becomes the limiting factor with precision of individual measurements frequently exceeding 3–5%. Nevertheless, the intensities of the low-abundance Pb isotopes are high enough even at 8 μm spot size when measured using IC device, suggesting further scope for improvement through special optimization.

Performance of two-volume HelEx-II sample ablation chamber

The newly designed two-volume HelEx-II sample cell is a large sample chamber that accommodates larger samples or multiple samples at a time, but effective volume of the sub-cell (cup) at the ablation site is only <2 cm^3 (ref. 23). This allows efficient aerosol transport using helium as carrier gas. The signal reaches 95% of peak intensity in ~1 sec after the laser is fired (Figure 1). Similarly, the washout time is also reduced to <2 sec to recede to <5% of peak value as against 7–12 sec in case of HelEx-I design[23] or other two-volume[24] or single, small-volume sample cell designs[25]. Such fast signal response and washout time in HelEx-II can reduce between sample washout times, thereby significantly improving sample throughput. However, we used 20 sec between sample intervals to ensure minimum memory effect.

Effect of spot size on down-hole fractionation

Laser-induced fractionation of heavier nuclides (^{238}U and ^{237}U) with respect to lighter ones (^{206}Pb and ^{207}Pb) is quite pronounced in static spot ablation[3,26,27], resulting in progressive increase in Pb/U ratios as the ablation proceeds. Fine homogeneous ablated particle size, an efficient aerosol transport and aspect ratio (spot diameter to depth ratio) >>1 are important considerations that can reduce isotopic fractionation.

Degree of down-hole fractionation was calculated as per cent change in 207/235 and 206/238 ratios between the signal time slice of 5th and 25th second of ablation. Degree of down-hole fraction for 207/235 and 206/238 is nearly identical and indistinguishable (Figure 2). Observed fractionation is ~11% only in case of larger spot size (35 μm). This is much less compared to a similar

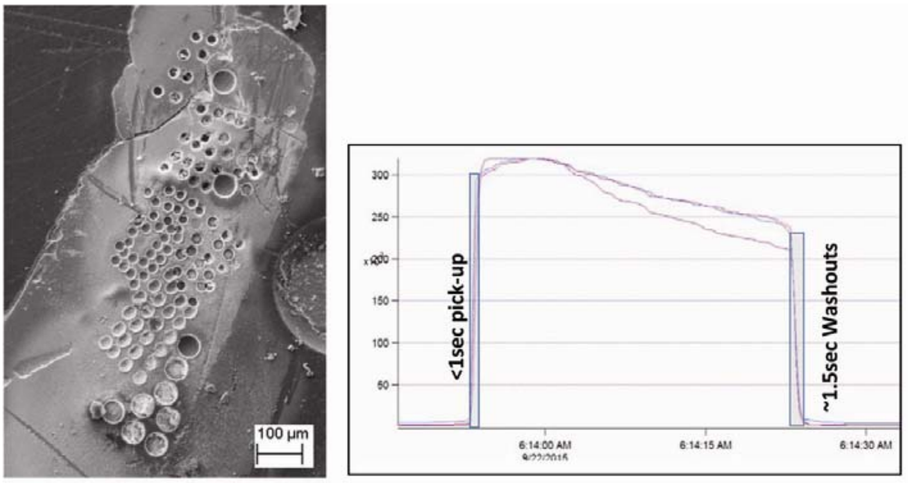

Figure 1. Typical laser ablation (LA) pits and time-series signal trace of ^{238}U and ^{206}Pb (intensity scale normalized) for a 30 sec single static measurement. Note the swift pick-up of signal reaching peak intensity in <1 sec of the laser-on and rapid washout of the signal to <1% of the peak intensity within 2 sec illustrating efficient transport and washout capability of the HelEx-II active two-volume ablation sample cell.

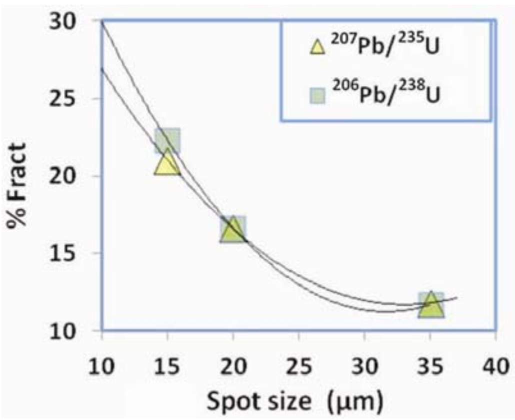

Figure 2. Degree of down-hole fractionation (%Fract) as a function of laser spot size showing increasing fractionation as the spot size is reduced or aspect ratio (spot dia/depth) reduces.

experiment with 35 µm spot size (~17%)[28] and 40 µm (20–30%)[29] for the same duration of ablation. Observed degree of fractionation increases with decreasing spot size and reaches up to 22% (Figure 2) in experiments using 15 µm spot size as the aspect ratio nearing unity. Use of Ar–F Excimer laser source, HelEx-II sample cell and higher aspect ratio (>1) resulted in very low degree of fractionation in the present case, which was readily corrected using off-line data processing through linear regression of the ratios measured for the reference sample as a function of depth profiling (or time) and is applied to the unknown samples alike according to standard practice.

Precision and accuracy

The results of the measurements are summarized in Table 2, that include precision (external) as %2σ (% standard error at 95% confidence level) error of mean of several cycles of measurements per analysis at a given spot size. Precision of isotopic ratio measurement is directly influenced by: (i) its abundance in the sample and ablation rate, (ii) instrumental sensitivity, and (iii) instrumental stability. This is reflected in the observed high precision of Plešovice zircon (U content 465–3084 ppm)[14] compared to Zircon 91500 (Figure 3 *a*), which contains an order of magnitude less U content (71–86 ppm)[13], while that of GJ-1 is moderate having intermediate U content (212–422 ppm). Similarly, for a particular zircon, highest precision is observed for larger spot size (35 µm) and it deteriorates as the spot size is reduced under constant laser fluence and repetition rate (Figure 3 *a*). Due to imprecision in measurement of lower abundance of $^{207}Pb^*$ compared to $^{206}Pb^*$ (ref. 16), the precision for $^{206}Pb/^{238}U$ ratio is always superior (<0.5% 2σ) compared to $^{207}Pb/^{235}U$ that reaches up to 0.8% (%2σ) for Plešovice and GJ-1 zircons irrespective of spot size, while for Harvard 91500 it is 1.17% for 20 µm and shoots up to 3.44% at 15 µm spot size.

Overall average external precision (2σ error) for 35 and 20 µm static ablation measurements for the final Pb/U ratios is <1% of the mean (Figure 3), while for 15 µm, it is considerably high, especially in case of Harvard 91500. These uncertainties in ratio measurement translate into final 2σ error in age of about ±7 Ma (<0.75%) in case of Harvard 91500 for spot sizes ≥20 µm. Corresponding error in age estimates for Plešovice is ± 2 Ma (<0.6%) and GJ-1 is ± 3 Ma (<0.6%) (Table 2 and Figure 3 *b*). In case of 15 µm experiment, the uncertainty for Plešovice and GJ-1 still remains below or ~1%, i.e. ±2.5 and ±6 Ma respectively, while that of Harvard 91500 is much higher (±19 Ma) but is still less than 2% error. Considering the complexity of natural zircons

Table 2. Summary statistics of the results for both ratio measurements and age estimates, for $^{207}Pb/^{235}U$ and $^{206}Pb/^{238}U$ geochronologic measurements at different LA spot sizes

	Spot size (μm)	91500 Final age 207/235	91500 Error 2σ Abs	91500 Final age 206/238	91500 Error 2σ Abs	PLSV Final age 207/235	PLSV Error 2σ Abs	PLSV Final age 206/238	PLSV Error 2σ Abs	GJ-1 Final age 207/235	GJ-1 Error 2σ Abs	GJ-1 Final age 206/238	GJ-1 Error 2σ Abs
Avg	35	1064.4	7.6	1063.5	8.29	337.4	2.1	337.7	1.6	601.6	3.0	600.8	2.6
% (2σ)	35		0.71		0.78		0.63		0.47		0.51		0.44
n	35	9		9		6		7		7		7	
Avg	20	1062.3	7.7	1060.9	7.2	337.9	2.0	336.0	1.4	600.3	3.7	593.4	2.7
% (2σ)	20		0.73		0.68		0.59		0.42		0.61		0.45
n	20	14		14		7		7		7		7	
Avg	15	1068.5	18.4	1067.5	18.9	340.5	2.5	339.1	1.3	598.8	6.9	596.9	4.4
% (2σ)	15		1.72		1.77		0.74		0.40		1.15		0.73
n	15	14		13		14		16		11		11	
	Spot size (μm)	91500 Final ratio 207/235	91500 Error 2σ Abs	91500 Final ratio 206/238	91500 Error 2σ Abs	PLSV Final ratio 207/235	PLSV Error 2σ Abs	PLSV Final ratio 206/238	PLSV Error 2σ Abs	GJ-1 Final ratio 207/235	GJ-1 Error 2σ Abs	GJ-1 Final ratio 206/238	GJ-1 Error 2σ Abs
Avg	35	1.8528	0.0214	0.1794	0.0015	0.3942	0.0028	0.0538	0.0003	0.8085	0.0055	0.0977	0.0004
% (2σ)	35		1.16		0.83		0.71		0.48		0.67		0.46
n	35	9		9		6		7		7		7	
Avg	20	1.8507	0.0216	0.1789	0.0013	0.3948	0.0027	0.0535	0.0002	0.8063	0.0065	0.0964	0.0005
% (2σ)	20		1.17		0.73		0.69		0.43		0.81		0.48
n	20	14		14		7		7		7		7	
Avg	15	1.8803	0.0647	0.1799	0.0038	0.3952	0.0036	0.0534	0.0002	0.8003	0.0123	0.0964	0.0008
% (2σ)	15		3.44		2.10		0.90		0.45		1.54		0.80
n	15	14		13		14		16		11		11	
D-TIMS reference values*													
Age		na	na	1062.32	2.22	337.24	0.33	337.14	0.27	601.59	3.80	599.75	4.82
Ratio	ID-TIMS	1.85013	0.00236	0.17916	0.00198	0.39403	0.00051	0.05368	0.00005	0.80930	0.00090	0.09761	0.00011

*Weidenberg *et al.*[13], for zircon 91500; Sláma *et al.*[14] for Plešovice zircon; Jackson *et al.*[11] for GJ-1 zircon.

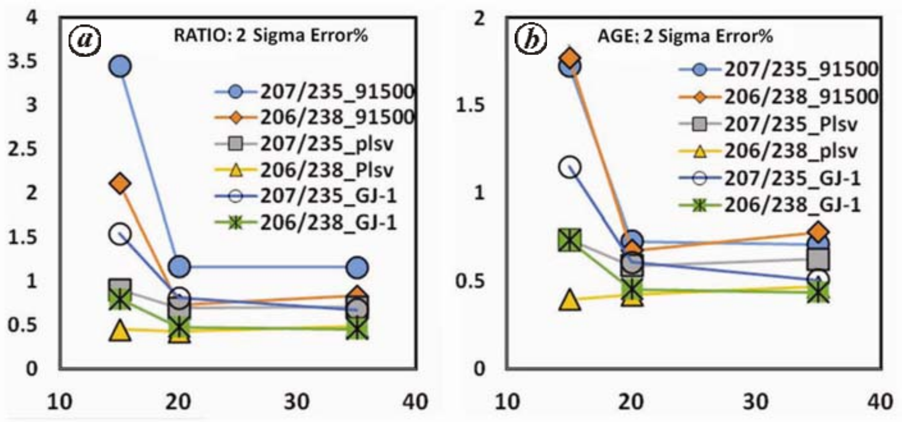

Figure 3. Precision of measurements of (***a***) ratio and (***b***) age represented as 2σ error (%) for different spot sizes.

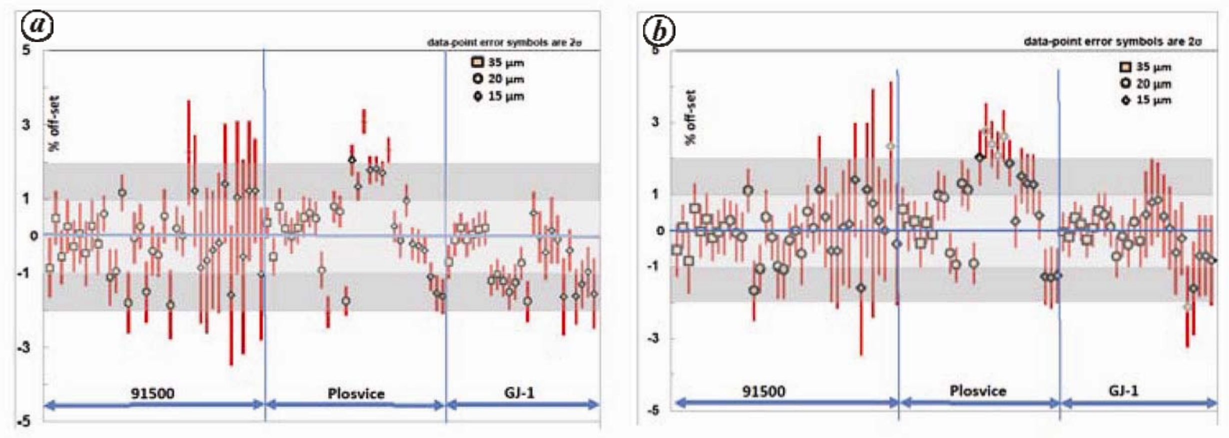

Figure 4. Weighted mean age offsets as %deviation with respect to the reference age for all the three reference samples, 91500, GJ-1 and Plešovice zircons. (***a***) $^{207}Pb/^{235}U$ and (***b***) $^{206}Pb/^{238}U$ ages. Grey shaded area represents ±1% and ±2% offset limits from the expected true values.

and low U content, these uncertainties of measurements are well within the acceptable limits. To this effect, Plešovice is a more suitable standard for high spatial resolution measurements than the Harvard 91500.

The accuracies of measurement are reported here as percentage offsets from the reference value (Figure 4). In comparison to $^{207}Pb/^{235}U$ ages, the accuracies of $^{206}Pb/^{238}U$ ages for all the three zircons are within ±1.5% of the reference value irrespective of spot sizes, with fewer exceptions. Excellent accuracies are observed for 35 and 20 μm experiments, which fall within ±1% 2σ error limit. In case of 15 μm spot size, however, mean age is comparable but with higher uncertainty of about ±2% of the reference value (Figure 4). These results are consistent and comparable with long-term statistics[30] under similar spot sizes and laser fluence experimental conditions. Compared to $^{207}Pb/^{235}U$ and $^{207}Pb/^{206}Pb$ ages, results of Plešovice zircon at 15 μm show greater offsets often exceeding 2% (±6 Ma) with respect to reference value (337 Ma). Yet the precision of these individual measurements is well within 0.5% (2σ error) due to higher U content. Overall for $^{207}Pb/^{235}U$ and $^{206}Pb/^{238}U$ ages measured for all the three zircon standard samples taken together at different spot sizes, the mean offset is found to be only –0.35%, with most of the individual values encompassed within ±2% offsets from the expected reference value (Figure 4).

Accuracy of measurement is also validated by the concordance of two U/Pb ages and illustrated by plots of the ratios $^{206}Pb/^{238}U$ versus $^{207}Pb/^{235}U$ on concordia diagram. The dimensions of the ellipse associated with each plot reveal the extent of uncertainty in measurement of the respective Pb/U isotopic ratio of an individual measurement (internal precision). The data points for all the three reference standard zircons are concordant and mostly cluster on the concordia line at the reference age (Figure 5). However, some data points show marginal discordance, especially data from the 15 μm experiment, but the degree of discordance is well within ±2% off set (Table 2). Although precision of measurements for Plešovice zircon at higher spatial resolution (15 μm) is excellent due to higher U content, the mean ages are a bit scattered

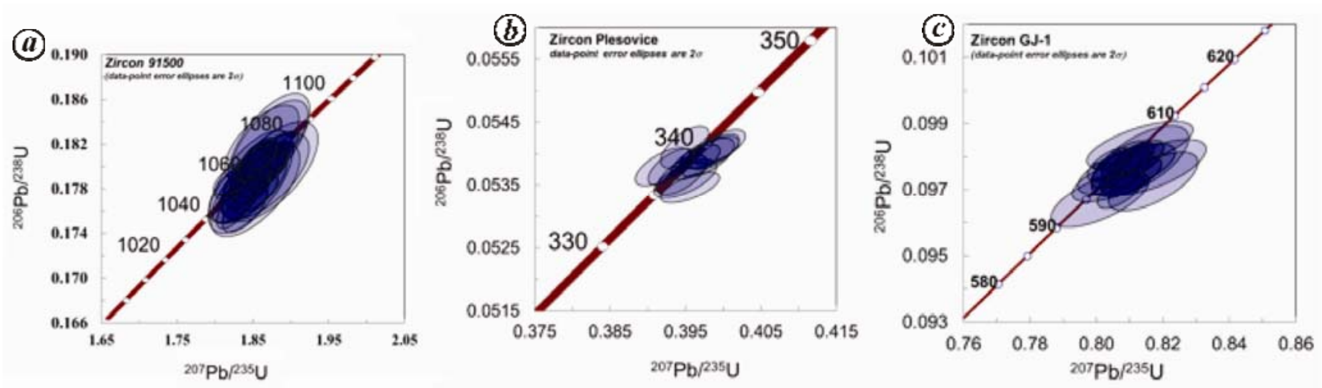

Figure 5. U–Pb Concordia diagram for zircon samples. (***a***) Harvard zircon 91500, (***b***) GJ-1 and (***c***) Plešovice at different static spot sizes (35, 20 and 15 μm).

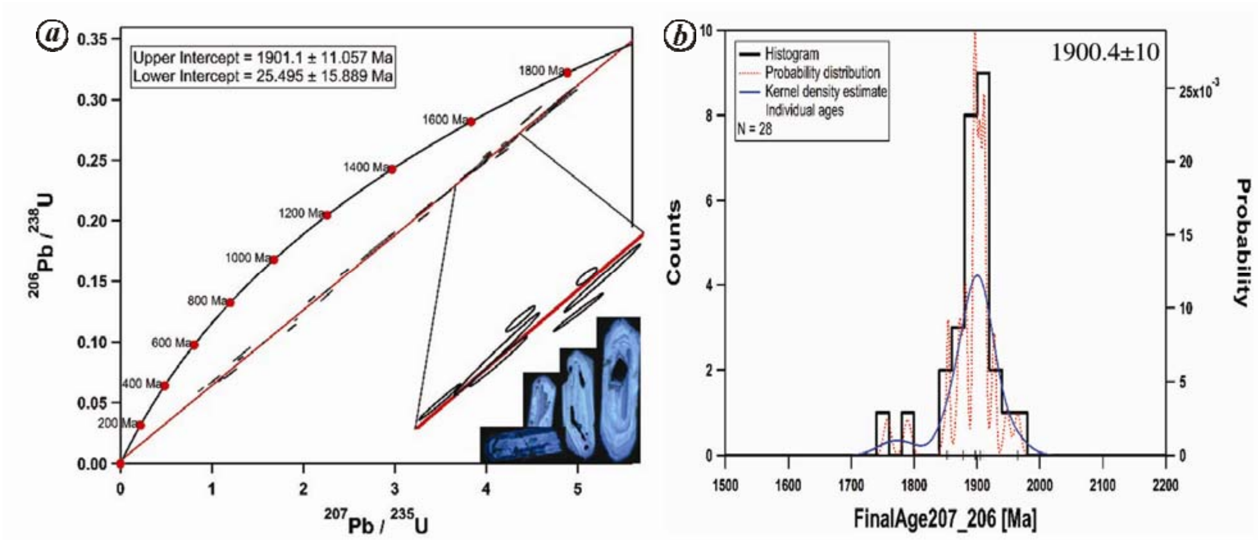

Figure 6. ^{206}Pb/^{238}U and ^{207}Pb/^{237}U concordia diagram for MCTZ zircon showing discordant plot due to extensive loss of radiogenic Pb due to later thermal event. Representative CL images showing igneous texture are shown in inset and magmatic crystallization age (1901 ± 11 Ma) is deduced from the upper intercept (***a***) or by clustering of ^{207}Pb–^{206}Pb ages (1900.4 ± 10) in the probability histogram (***b***).

(~±2.4%). In view of the higher spatial resolution, these offsets are quite reasonable (cf. ref. 14). Further, Plešovice zircons are known to have occasional mineral inclusions (apatite, K-feldapar and patches of high actinides) that may affect the analysis if appropriate attention is not paid to avoid such anomalous zones.

Zircon geochronology of gneissic mylonite from MCTZ

Munsiari Formation, also referred to as MCTZ, occurs immediately in contact with the Higher Himalayan Crystallines and the thrust contact is referred to as MCT or Vaikrita Thrust[31]. Typical augen gneissic mylonites of Munsiari Formation of the inner Lesser Himalaya have been subjected to U–Pb dating of detrital zircons by many workers[32,33] and an age range of 1850–1950 Ma has been suggested independently by these workers. An intensely deformed mylonitic gneissic sample was collected from this Formation at Joshimath on the foot wall of the MCT for zircon geochronology as a test sample. The zircons are sufficiently enriched but variable in U content with an average of 570 ppm compared to Th (U/Th ratio >9.5), suggesting that the zircons are igneous in origin and were derived from magmatic source. Internal precision of corrected U/Pb isotopic ratio measurement is well within 1%. The results of the study show that the ^{206}Pb/^{238}U and ^{207}Pb/^{235}U ages from rim as well as core are highly discordant, but define a clear trend with an upper intercept at 1901 ± 11 Ma and a lower incept at 25 ± 16 Ma on the concordia plot (Figure 6 *a*). Inherent older (late Achaean) core observed in a few grains has been excluded from the concordia plot. The upper intercept age is inferred here as the magmatic crystallization age, while the lower intercept age may be considered as recent tectonothermal event leading to lead loss. Further, it is also observed that the weighted mean of $^{207}Pb/^{206}Pb$ ages (1900.4 ± 10) (Figure 6 *b*) converges with the upper-intercept age. Though the lower intercept at 25 ± 16 Ma has much higher uncertainty rendering it meaningless. This loss event during late Oligocene–early Miocene coincides with the timing of tectono-thermal activities along the MCT leading to intense ductile deformation and mylonitization[34]. Further studies are required, especially targeting the thin overgrowth rim of these zircons for U–Pb dating. The palaeo-proterozoic magmatic age obtained in this study is consistent with the published dates[30,32].

Conclusion

This study evaluated analytical results of U–Pb microgeochronology of zircon using LA with mixed detector MC-ICPMS configuration. Stability of the MC-ICPMS instrumentation and precision of measurements are well demonstrated by replicate analyses of well-characterized reference standards (Harvard 91500, GJ-1 and Plešovice) at different spatial resolutions. The two-volume HelEx-II active ablation cell provides unmatched signal pick-up and washout time (<2 sec) characteristics and stability. With careful optimization of analytical conditions, reasonable precision and accuracy of zircon dating can be achieved even at resolutions less than 15 μm.

U–Pb dating of zircons can be achieved with a reasonably high external precision of ~0.71% at 95% confidence at an optimum spot size of ≥20 μm. Spot size smaller than 20 μm shows rapid degradation of precision (~1.7% 2σ error), especially for U-poor zircons. Accuracies validated as offset (%) with respect to the reference value are generally well within 1% for ≥20 μm spot size, while for 15 μm or less, it occasionally exceeds 1.5%–2%. Reasonable precision can also be expected at smaller spot sizes if the zircon is suitably enriched in U.

The igneous zircons from the footwall of the MCT (i.e. Munsiari Formation) of the inner Lesser Himalaya yield magmatic crystallization age of 1901 ± 11 Ma with internal precision for individual measurements well within 1%. A late Oligocene–early Miocene thermal phase of extensive radiogenic Pb-loss in zircons is also inferred from the lower intercept of highly discordant array of U/Pb concordia plots on. Except for a few grains with late Achaean older inherited core, the rim and core of the zircons show very consistent palaeo-Proteriozoic magmatic age.

1. Gunther, D., Frischknecht, R., Heinrich, C. A. and Kahlert, H. J., Capabilities of an argon fluoride 193 nm excimer laser for laser ablation inductively coupled plasma mass Spectrometry microanalysis of geological materials. *J. Anal. At. Spectrom.*, 1997, **12**(9), 939–944.
2. Günther, D. and Heinrich, C. A., Enhanced sensitivity in laser ablation-ICP mass spectrometry using helium-argon mixtures as aerosol carrier. *J. Anal. At. Spectrom.*, 1999, **14**(9), 1363–1368.
3. Jackson, S. E., Pearson, N. J., Griffin, W. L. and Belousova, E. A., The application of laser ablation-inductively coupled plasma-mass spectrometry to *in situ* U–Pb zircon geochronology. *Chem. Geol.*, 2004, **211**(1), 47–69.
4. Simonetti, A., Heaman, L. M., Chacko, T. and Banerjee, N. R., *In situ* petrographic thin section U–Pb dating of zircon, monazite, and titanite using laser ablation–MC–ICP–MS. *Int. J. Mass Spectrom.*, 2006, **253**(1), 87–97.
5. Sylvester, P. J. (ed.), *Laser Ablation–ICP-MS in the Earth Sciences: Current Practices and Outstanding Issues*, Mineralogical Association of Canada Short Course Series, 2008, vol. 40, p. 348.
6. Walder, A. J., Koller, D., Reed, N. M., Hutton, R. C. and Freedman, P. A., Isotope ratio measurements by inductively coupled plasmamultiple collector-mass spectrometry incorporating a high efficiency nebulization system. *J. Anal. At. Spectrom.*, 1993, **8**, 1037–1041.
7. Albarede, F., Telouk, P., Blichert-Toft, J., Boyet, M., Agranier, A. and Nelson, B., Precise and accurate isotopic measurements using multiple-collector ICPMS. *Geochim. Cosmochim. Acta*, 2004, **68**(12), 2725–2744.
8. Hinton, R. W. and Upton, B. G. J., The chemistry of zircon: variations within and between large crystals from syenite and alkali basalt xenoliths. *Geochim. Cosmochim. Acta*, 1991, **55**, 3287–3302.
9. Buick, R., Thornett, J. R., McNaughton, N. J., Smith, J. B., Barley, M. E. and Savage, M., Record of emergent continental crust ~3.5 billion years ago in the Pilbara Craton of Australia. *Nature*, 1995, **375**(6532), 574–577.
10. Maas, R., Kinny, P. D., Williams, I. S., Froude, D. O. and Compston, W., The Earth's oldest known crust: a geochronological and geochemical study of 3900–4200 Ma old detrital zircons from Mt. Narryer and Jack Hills, Western Australia. *Geochim. Cosmochim. Acta*, 1992, **56**, 1281–1300.
11. Jackson, S. E., Pearson, N. J., Griffin, W. L. and Belousova, E. A., The application of laser ablation-inductively coupled plasma-mass spectrometry to *in situ* U–Pb zircon geochronology. *Chem. Geol.*, 2004, **211**, 47–69.
12. Chang, Z., Vervoort, J. D., McClelland, W. C. and Knaack, C., U–Pb dating of zircon by LA-ICP-MS. *Geochem. Geophys. Geosyst.*, 2006, **7**(5), 1–14.
13. Wiedenbeck, M. *et al.*, Three natural zircon standards for U–Th–Pb, Lu–Hf, trace element and REE analyses. *Geostand. Newsl.*, 1995, **19**, 1–23.
14. Sláma, J. *et al.*, Plešovice zircon – a new natural reference material for U–Pb and Hf isotopic micro-analysis. *Chem. Geol.*, 2008, **249**, 1–35.
15. Spencer, C. J., Kirkland, C. L. and Taylor, R. J., Strategies towards statistically robust interpretations of in situ U–Pb zircon geochronology. *Geosci. Front.*, 2015; http://dx.doi.org/10.1016/j.gsf.2015.11.006.
16. Gehrels, G., Detrital zircon U–Pb geochronology: current methods and new opportunities. In *Tectonics of Sedimentary Basins: Recent Advances* (eds Busby, C. and Azor, A.), John Wiley, Chichester, UK, 2011, pp. 45–62; doi: 10.1002/9781444347166.ch2.
17. Jaffey, A. H., Flynn, K. F., Glendenin, L. E., Bentley, W. C. and Essling, A. M., Precision measurement of half-lives and specific activities of ^{235}U and ^{238}U. *Phys. Rev.*, 1971, **C4**, 1889–1906.
18. Mattinson, J. M., Analysis of the relative decay constants of ^{235}U and ^{238}U by multi-step CA-TIMS measurements of closed-system natural zircon samples. *Chem. Geol.*, 2010, **275**, 186–198.
19. Hiess, J., Condon, D. J., McLean, N. and Noble, S. R., $^{238}U/^{235}U$ systematics in terrestrial uranium-bearing minerals. *Science*, 2012, **335**(6076), 1610–1614.
20. Paton, C., Hellstrom, J., Paul, B., Woodhead, J. and Hergt, J., Iolite: Freeware for the visualisation and processing of mass

spectrometric data. *J. Anal. At. Spectrom.*, 2011, **26**(12), 2508–2518.

21. Petrus, J. A. and Kamber, B. S., VizualAge: a novel approach to laser ablation ICP-MS U–Pb geochronology data reduction. *Geostand. Geoanal. Res.*, 2012, **36**, 247–270.
22. Ludwig, K. R., Isoplot/Ex Version 3.00: a geochronological toolkit for Microsoft Excel. Special Publication No. 4, Berkeley Geochronology Center, Berkeley, USA, 2003.
23. Woodhead, J. D., Hellstrom, J., Hergt, J. M., Greig, A. and Maas, R., Isotopic and elemental imaging of geological materials by laser ablation inductively coupled plasma-mass spectrometry. *Geostand. Geoanal. Res.*, 2007, **31**(4), 331–343.
24. Solari, L. A., Gómez-Tuena, A., Bernal, J. P., Pérez-Arvizu, O. and Tanner, M., U–Pb zircon geochronology with an integrated LA-ICP-MS microanalytical workstation: achievements in precision and accuracy. *Geostand. Geoanal. Res.*, 2010, **34**(1), 5–18.
25. Fryer, B. J., Jackson, S. E. and Longerich, H. P., The design, operation and role of the laserablation microprobe coupled with an inductively coupled plasma; mass spectrometer (LAM–ICP–MS) in the earth sciences. *Can. Mineral*., 1995, **33**(2), 303–312.
26. Eggins, S. M., Kinsley, L. P. J. and Shelley, J. M. M., Deposition and elemental fractionation processes during atmospheric pressure laser sampling for analysis by ICP-MS. *Appl. Surf. Sci.*, 1998, **127/129**, 278–286.
27. Mank, A. J. G. and Mason, P. R. D., A critical assessment of laser ablation ICP-MS as an analytical tool for depth analysis in silica-based glass samples. *J. Anal. At. Spectrom*., 1999, **14**, 1143–1153.
28. Horn, I., Rudnick, R. L. and McDonough, W. F., Precise elemental and isotope ratio determination by simultaneous solution nebulization and laser ablation-ICP-MS: application to U–Pb geochronology. *Chem. Geol.*, 2000, **164**(3), 281–301.
29. Paton, C., Woodhead, J. D., Hellstrom, J. C., Hergt, J. M., Greig, A. and Maas, R., Improved laser ablation U-Pb zircon geochronology through robust down-hole fractionation correction. *Geochem. Geophys. Geosyst*., 2010, **11**, Q0AA06; doi:10.1029/2009GC002618.
30. Gehrels, G. E., Valencia, V. A. and Ruiz, J., Enhanced precision, accuracy, efficiency, and spatial resolution of U–Pb ages by laser ablation-multicollectorinductively coupled plasma-mass spectrometry. *Geochem. Geophys. Geosyst.*, 2008, **9**, Q03017.
31. Valdiya, K. S., *Geology of Kumaun Lesser Himalaya*, Wadia Institute of Himalayan Geology, Dehradun, 1980.
32. Gehrels, G. *et al.*, Detrital zircon geochronology of pre-Tertiary strata in the Tibetan-Himalayan orogen. *Tectonics*, 2011, **30**, 27; doi:10.1029/2011TC002868.
33. Spencer, C. J., Harris, R. A. and Dorais, M. J., Depositional provenance of the Himalayan metamorphic core of Garhwal region, India: Constrained by U–Pb and Hf isotopes in zircons. *Gondwana Res.*, 2012, **22**(1), 26–35.
34. Johnson, M. R. W., Oliver, G. J. H., Parrish, R. R. and Johnson, S. P., Synthrusting metamorphism, cooling, and erosion of the Himalayan Kathmandu complex. *Tectonics*, 2001, **20**, 394–415.

ACKNOWLEDGEMENTS. We thank the Director, Wadia Institute of Himalayan Geology (WIHG), Dehra Dun for his efforts in establishing the state-of-the-art micro-geochronology facility (LA–MC–ICPMS) though special financial assistance from the Department of Science and Technology (DST), New Delhi. A. K. Jain has been the driving force and constant source of encouragement. P. P. Khanna, N. K. Saini, A. K. Singh, H. K. Sachan, M. K. Panigrahi and S. C. Patel helped us in establishing the facility. We also thank Dr Nick Lloyd (Thermo Fisher Scientific) and Dr Ciprian Stremtan (Teledyne) for their help in setting-up the Laser Ablation mode for U–Pb dating. We also thank all those in WIHG who have contributed directly or indirectly in establishing this micro-geochronology facility.

Received 28 June 2016; revised accepted 25 October 2016

doi: 10.18520/cs/v112/i04/802-810